Optimized Dispatching Method for Flexibility Improvement of AC-MTDC Distribution Systems Considering Aggregated Electric Vehicles

Xingyue Jiang, Shouxiang Wang, *Senior Member*, *IEEE*, Qianyu Zhao, and Xuan Wang

***Abstract*—With the increasing use of renewable resources and electric vehicles (EVs), the variability and uncertainty in their nature put forward a high requirement for flexibility in AC distribution system incorporating voltage source converter (VSC) based multi-terminal direct current (MTDC) grids. In order to improve the capability of distribution systems to cope with uncertainty, the flexibility enhancement of AC-MTDC distribution systems considering aggregated EVs is studied. Firstly, the charging and discharging model of one EV is proposed considering the users' demand difference and traveling needs. Based on this, a vehicle-to-grid (V2G) control strategy for aggregated EVs to participate in the flexibility promotion of distribution systems is provided. After that, an optimal flexible dispatching method is proposed to improve the flexibility of power systems through cooperation of VSCs, controllable distributed generations (CDGs), aggregated EVs, and energy storage systems (ESSs). Finally, a case study of an AC-MTDC distribution system is carried out. Simulation results show that the proposed dispatching method is capable of effectively enhancing the system flexibility, reducing renewable power curtailment, decreasing load abandonment, and cutting down system cost.**

***Index Terms*—Multi-terminal direct current (MTDC), distribution system, aggregated electric vehicles (EVs), flexibility, optimized dispatching.**

NOMENCLATURE

A. Parameters

μ	Coefficient related to modulation mode
$\eta_{ev,i}^{chg}$, $\eta_{ev,i}^{dis}$	Charging and discharging efficiencies of electric vehicle (EV) i
Ω_{AC}, Ω_{DC}, Ω_{LD}	Sets of AC lines, DC lines, and loads
Ω_{chg}, Ω_{sfi}, Ω_{dis}	Sets of charging, shiftable charging, and discharging EVs
Ω_{sys}, Ω_{WT}, Ω_{PV}, Ω_{CDG}, Ω_{ESS}, Ω_{EVA}	Sets of sub-grids, wind turbines (WTs), photovoltaic (PV) units, controllable distributed generations (CDGs), energy storage systems (ESSs), and EV aggregators (EVAs)
$\Psi_S(j)$, $\Psi_G(j)$, $\Psi_W(j)$, $\Psi_P(j)$, $\Psi_E(j)$, $\Psi_A(j)$, $\Psi_L(j)$, $\Psi_V(j)$	Sets of sub-grids, CDGs, WTs, PV units, ESSs, EVAs, loads, and voltage source converters (VSCs) connected to AC bus j
$\Psi_G^d(j)$, $\Psi_W^d(j)$, $\Psi_P^d(j)$, $\Psi_E^d(j)$, $\Psi_A^d(j)$, $\Psi_L^d(j)$, $\Psi_V^d(j)$	Sets of CDGs, WTs, PV units, ESSs, EVAs, loads, and VSCs connected to DC bus j
$c_{CDG,i}$, $c_{CDG,i}^{up}$, $c_{CDG,i}^{dn}$	Operation, start-up, and shut-down costs of CDG i
$c_{ev,sfi}$, $c_{ev,dis}$	Compensation costs of shiftable charging EVs and discharging EVs
c_{WT}, c_{PV}, c_{ESS}	Maintenance costs of WTs, PV units, and ESSs
$c_{WT,psh}$, $c_{PV,psh}$, $c_{LD,psh}$	Penalty costs for involuntary power abandonment of WTs, PV units, and loads
$C_{ev,i}^{cnv,\max}$	The maximum charge-discharge switching number of EV i
$C_{WT,opr}$, $C_{PV,opr}$, $C_{CDG,opr}$, $C_{ESS,opr}$	Operation costs of WT, PV unit, CDG, and ESS
$C_{EVA,comp}$	Compensation cost of EVA
$C_{WT,psh}$, $C_{PV,psh}$, $C_{LD,psh}$	Punishment costs of power curtailment of WT, PV unit, and load
$E_{ev,i}$	Energy capacity of EV i
G_{ij}, B_{ij}	Conductance and susceptance of AC line connecting AC buses i and j
G_{ij}^d	Conductance of DC line connecting DC buses i and j
$M_{VSC,i}$	Modulation index of VSC i
$P_{ev,i}^{chg,rt}$, $P_{ev,i}^{dis,rt}$	Rated charging and discharging power of EV i
$P_{VSC,i}^{ref}$, $Q_{VSC,i}^{ref}$	Active and reactive power references of VSC i

Manuscript received: September 8, 2022; revised: December 10, 2022; accepted: March 14, 2023. Date of CrossCheck: March 14, 2023. Date of online publication: May 1, 2023.

This work was supported in part by the National Natural Science Foundation of China (No. U2166202) and S&T Program of Hebei (No. 20312102D).

X. Jiang, S. Wang, Q. Zhao (corresponding author), and X. Wang are with the Key Laboratory of Smart Grid of Ministry of Education, Tianjin University, Tianjin 300072, China (e-mail: xyjiang@tju.edu.cn; sxwang@tju.edu.cn; zhaoqianyu@tju.edu.cn; tjdxwx@tju.edu.cn).

DOI: 10.35833/MPCE.2022.000576

$Q_{VSC,i}^{\max}$, $Q_{VSC,i}^{\min}$ The maximum and minimum reactive power limits of VSC i

r_{ij}, r_{ij}^{d} Resistance of AC branch ij and DC branch ij

$SOC_{ev,i}^{\max}$ The maximum state of charge (SOC) of EV i

$SOC_{ev,i}^{exp}$, $SOC_{ev,i}^{thd}$ Expected SOC and discharging threshold of SOC of EV i

$S_{line,i}^{\max}$, $S_{trsf,i}^{\max}$, $S_{VSC,i}^{\max}$ The maximum transfer capacities of line i, transformer i, and VSC i

T Number of dispatching intervals

ΔT Dispatching interval

$T_{ev,i}^{leav}$ Expected departure time of EV i

$T_{ev,i}^{chg,req}$ The minimum time required for shiftable EV i to be charged to the expected SOC with constant power from time t

$T_{ev,i}^{dis,req}$ The minimum charging time required to meet EV user's traveling needs if schedulable EV i discharges at time t

$V_{VSC,i}^{ref}$, $V_{VSC,i}^{d,ref}$ Voltage references of AC bus and DC bus connecting to VSC i

B. Variables

$\theta_{ij}(t)$ Voltage angle difference between AC buses i and j at time t

$\alpha_{ev,i}^{chg}(t)$, $\alpha_{ev,i}^{dis}(t)$, $\alpha_{ESS,i}^{chg}(t)$, $\alpha_{ESS,i}^{dis}(t)$ Charging and discharging state variables of EV i and ESS i at time t

$\alpha_{ev,i}^{sft}(t)$, $\alpha_{ev,i}^{sg}(t)$ Shifting state variable and shifting signal of shiftable EV i

$\alpha_{CDG,i}^{up}(t)$, $\alpha_{CDG,i}^{dn}(t)$ Start-up and shut-down state variables of CDG i at time t

$\alpha_{ev,i}^{sgdis}(t)$ Discharging signal of schedulable EV i

$c_{Grid,i}(t)$ Time-varying electricity price of grid i at time t

$F_{de}^{up}(t)$, $F_{de}^{dn}(t)$ System upward and downward flexibility demands at time t

$F_{EVA,i}^{up}(t,\Delta T)$, $F_{EVA,i}^{dn}(t,\Delta T)$ Upward and downward flexibility supplies of EVA i at time t

$F_{SA}^{up}(t)$, $F_{SA}^{dn}(t)$ Upward and downward flexibility supplies of AC-MTDC distribution system at time t

$F_{sup,rev}^{up}(t,\Delta T)$, $F_{sup,rev}^{dn}(t,\Delta T)$ System upward and downward flexibility reserves at time t

$F_{sup}^{up}(t,\Delta T)$, $F_{sup}^{dn}(t,\Delta T)$ The maximum upward and downward flexibility supplies of AC-MTDC distribution system at time t

$FSA(t)$, $NTM(t)$ Flexibility supply adequacy (FSA) and network transfer margin (NTM) at time t

$I_{ij}(t)$, $I_{ij}^{d}(t)$ Currents of AC branch ij and DC branch ij at time t

$P_{CDG,i}(t)$, $Q_{CDG,i}(t)$ Active and reactive power outputs of CDG i at time t

$P_{ev,i}^{chg}(t)$, $P_{ESS,i}^{chg}(t)$, $P_{ev,i}^{dis}(t)$, $P_{ESS,i}^{dis}(t)$ Charging and discharging power of EV i and ESS i at time t

$P_{EVA,i}^{chg}(t)$, $P_{EVA,i}^{dis}(t)$ Charging and discharging power of EVA i at time t

$P_{Grid,i}(t)$, $Q_{Grid,i}(t)$ Active and reactive power purchased from the upper-level grid i at time t

$P_{j}^{inj}(t)$, $Q_{j}^{inj}(t)$ Active and reactive power injected into AC bus j at time t

$P_{j}^{d,inj}(t)$ Active power injected into DC bus j at time t

$P_{LD}(t)$, $Q_{LD}(t)$ Active and reactive power of load i at time t

$P_{NL}(t)$ Net load at time t

$P_{VSC,i}(t)$, $Q_{VSC,i}(t)$ Active and reactive power of VSC i at time t

$P_{WT,i}(t)$, $P_{PV,i}(t)$ Active power of WT i and PV unit i at time t

$\Delta P_{WT,i}(t)$, $\Delta P_{PV,i}(t)$, $\Delta P_{LD,i}(t)$ Involuntary curtailments of WT i, PV unit i, and load i at time t

$SOC_{ev,i}(t)$ SOC value of EV i at time t

$SOC_{ev,i}^{chg}(t+\Delta T)$ SOC value of EV i being charged with constant power from time t to ΔT

$S_{line,i}(t)$, $S_{trsf,i}(t)$, $S_{VSC,i}(t)$ Transfer capacities of line i, transformer i, and VSC i at time t

$S_{SA}^{up}(t)$, $S_{SA}^{dn}(t)$ State variables of upward and downward FSA at time t

$V_{i}(t)$, $V_{i}^{d}(t)$ Voltage values of AC bus i and DC bus i at time t

$V_{VSC,i}(t)$, $V_{VSC,i}^{d}(t)$ AC and DC bus voltages of VSC i at time t

I. Introduction

THE increasing utilization of renewable energy resources and electric vehicles (EVs) imposes significant challenges on distribution system operation [1]. In order to operate safely and reliably, distribution systems are required to be flexible enough to cope with variability and uncertainty in both generation and demand sides [2]. The AC distribution system incorporating voltage source converter (VSC) based multi-terminal direct current (MTDC) grids can be a development direction and strategic choice for future distribution systems [3]. How to reduce renewable power curtailment and make AC-MTDC distribution systems more flexible has become one of the hot spots in power systems.

System flexibility is the ability of power systems to respond to unexpected changes and has received extensive attention in recent years [4]-[10]. The literature on the concepts, indexes, and implementation of flexibility in power system security was surveyed in [4]. Various flexible resources such as flexible generators [5], demand response [6], energy storage systems (ESSs) [7], microgrids [8], network reconfiguration [9], and even efficient system operations [10]

are capable of improving power system flexibility. To evaluate the flexibility in power systems, extensive researches were carried out [11]-[14]. The concept of flexibility envelope was presented in [11]. Some flexibility indexes are developed to assess how flexible a power system is. Probabilistic evaluation indexes such as insufficient ramping resource expectation (IRRE), periods of flexibility deficit (PFD) [12], and lack of ramp probability (LORP) [13] are able to show the probability of flexibility shortage. However, these indexes fail to reflect the information of curtailment. In [14], flexibility supply adequacy (FSA) and network transfer margin (NTM) were provided to assess the system flexibility.

With more and more uncertainties in the grid, it has become an inevitable trend to consider flexibility in power system scheduling [15]-[19]. An economic dispatching was introduced in [15] which took battery storage as a flexible resource to promote system flexibility. A centralized scheduling model was developed in [16] to exploit demand flexibility from residential devices. Moreover, [17]-[19] concentrated on the economic dispatching of power systems with various kinds of flexible resources. However, the aforementioned studies are generally based on AC power systems. As for the AC/DC hybrid systems, a multi-objective flexible and economic scheduling of AC/DC distribution systems was presented in [20] taking the uncertainty of wind power into account. In [21], an integrated optimization approach was proposed to exploit the operational flexibility of generation, high-voltage direct current (HVDC), and transmission switching in wind integrated AC/DC hybrid systems. Moreover, an optimal dispatching model was provided in [14] to improve the system flexibility through VSC regulation, MTDC mode switching, and flexible resource collaboration in AC-MTDC distribution system.

With the popularity of EVs, the increasing penetration of EVs has made a profound influence on the security and stability of distribution systems. To accurately reflect the charging characteristics of EVs, EV charging and discharging model should incorporate factors such as battery type, travel need, and user behavior [22], [23]. A general charging model of EVs was provided in [22] considering battery type, driving pattern, and user charging behavior. User's travel plan and own energy consumption behavior were considered in [23]. However, these studies only deal with the charging model of EVs. The charging and discharging model of EVs was controlled according to state of charge (SOC) of EV battery and EV owners' driving requirements in [24]. Besides, slow charging and fast charging EVs were modeled through six operating modes in [25]. However, EV users' demand differences have not been considered in the aforementioned EV models. In actual scenarios, EV users can choose whether to take part in demand response or not, and select any type of demand response to participate in according to their willingness. Thus, there is an inevitable contradiction between existing research and actual scene.

Orderly management of EV charging and discharging process can realize a friendly interaction between EVs and the grid [26]-[31]. A power smoothing service was developed in [26] to mitigate undesirable fluctuations of wind power. A strategy was provided in [27] to guide the charging and discharging of EVs in peak-load reduction and valley filling in an orderly manner. In addition, [28]-[30] studied the participation of EVs in voltage control, frequency regulation, and system reserve, respectively.

The coordinated dispatching problem of EVs in distribution systems is of great importance and has been studied by many research works [31]-[37]. Optimal dispatching strategies of EVs were proposed to maximize the benefit of EV users or EV aggregators (EVAs) in [31] and [32]. Dynamic electricity prices were used in [33] to guide the charging and discharging behavior of EVs during the optimization dispatching. Moreover, optimal dispatching methods coordinating the operations of EVs were provided in [34]-[36] to reduce load shedding and renewable power curtailment in distribution systems. In order to alleviate the burden of computation, the optimal operation of power grid and EVAs in a coordinative manner was carried out in [37].

From the above analysis, it is clear that the research on aggregated EVs to take part in the flexibility enhancement of AC-MTDC distribution systems has not been carried out. Besides, the charging and discharging model of single EV needs to be improved to incorporate demand differences of EV owners. Meanwhile, the vehicle-to-grid (V2G) strategy for aggregated EVs to provide flexibility supply requires to be formulated. To this end, this paper concentrates on the problem of improving the flexibility of AC-MTDC distribution systems considering aggregated EVs. The main contributions of the paper are highlighted as follows.

1) The charging and discharging model of one EV considering user's demand differences is established. Then plug-in EVs can be divided into rigid EVs, shiftable EVs, and schedulable EVs.

2) The V2G control strategy is developed for aggregated EVs to participate in demand response to promote the ability of AC-MTDC distribution system to respond to unexpected changes.

3) Taking two flexibility evaluation indexes into account, an optimal flexible scheduling model of AC-MTDC distribution system is established considering controllable distributed generations (CDGs), ESSs, aggregated EVs, and VSCs.

The remainder of this paper is organized as follows. Section II describes the control model of a single EV and establishes a V2G strategy for aggregated EVs. Section III discusses the optimal flexible dispatching of AC-MTDC distribution systems considering CDGs, ESSs, aggregated EVs, and VSCs. Case study is provided in Section IV to show the merits and effectiveness of the proposed method. Section V gives the conclusion.

II. Control Model of Single EV and V2G Strategy for Aggregated EVs

A. Charging and Discharging Model of Single EV

The dispatching center enables EV owners to actively participate in various types of demand responses. Then, EV users can choose to take part in any type of demand response. According to EV owners' participation willingness, plug-in

EVs can be refined into three types, namely rigid EVs, shiftable EVs, and schedulable EVs. Charging and discharging models of various types of EVs are given as follows.

1) Rigid EVs

Rigid EVs are charged as soon as they are plugged in until their expected SOCs are reached. The charging power of rigid EV i at any time t can be determined by:

$$\begin{cases} P_{ev,i}^{chg}(t)=P_{ev,i}^{chg,rt} & SOC_{ev,i}^{chg}(t+\Delta T)\le SOC_{ev,i}^{exp} \\ P_{ev,i}^{chg}(t)\in(0,P_{ev,i}^{chg,rt}) & SOC_{ev,i}^{chg}(t+\Delta T)>SOC_{ev,i}^{exp} \end{cases} \tag{1}$$

Formula (1) represents that rigid EV i is charged with $P_{ev,i}^{chg}(t)$ until it leaves the grid. $SOC_{ev,i}^{chg}(t+\Delta T)$ can be determined by:

$$SOC_{ev,i}^{chg}(t+\Delta T)=SOC_{ev,i}(t)+\eta_{ev,i}^{chg}P_{ev,i}^{chg,rt}\Delta T/E_{ev,i} \tag{2}$$

2) Shiftable EVs

Shiftable EVs do not feed power into the grid, but their charging power can be shifted to other scheduling time intervals according to shifting signals from EVAs. The charging power of shiftable EV i at time t can be given by:

$$\begin{cases} P_{ev,i}^{chg}(t)=(1-\alpha_{ev,i}^{sft}(t)\alpha_{ev,i}^{sg}(t))P_{ev,i}^{chg,rt} & SOC_{ev,i}^{chg}(t+\Delta T)\le SOC_{ev,i}^{exp} \\ P_{ev,i}^{chg}(t)\in[0,P_{ev,i}^{chg,rt}) & SOC_{ev,i}^{chg}(t+\Delta T)>SOC_{ev,i}^{exp} \end{cases} \tag{3}$$

Considering EV owners' traveling needs, the following conditions must be satisfied:

$$\alpha_{ev,i}^{sft}(t)=\begin{cases} 1 & T_{ev,i}^{chg,req}<T_{ev,i}^{leav}-t-\Delta T \\ 0 & T_{ev,i}^{chg,req}\ge T_{ev,i}^{leav}-t-\Delta T \end{cases} \tag{4}$$

$T_{ev,i}^{chg,req}$ can be calculated by:

$$T_{ev,i}^{chg,req}=(SOC_{ev,i}^{exp}-SOC_{ev,i}(t))E_{ev,i}/(\eta_{ev,i}^{chg}P_{ev,i}^{chg,rt}) \tag{5}$$

3) Schedulable EVs

Schedulable EVs can either inject power into the grid or shift their charging loads if needed during connected periods. They can be treated as shiftable EVs under charging state. Schedulable EV i can inject power into the grid once it satisfies:

$$P_{ev,i}^{dis}(t)=\begin{cases} \alpha_{ev,i}^{dis}(t)\alpha_{ev,i}^{sgdis}(t)P_{ev,i}^{dis,rt} & SOC_{ev,i}(t)>SOC_{ev,i}^{thd} \\ 0 & SOC_{ev,i}(t)<SOC_{ev,i}^{thd} \end{cases} \tag{6}$$

$$\alpha_{ev,i}^{dis}(t)=\begin{cases} 1 & T_{ev,i}^{dis,req}<T_{ev,i}^{leav}-t-\Delta T \\ 0 & T_{ev,i}^{dis,req}\ge T_{ev,i}^{leav}-t-\Delta T \end{cases} \tag{7}$$

$T_{ev,i}^{dis,req}$ can be determined by:

$$T_{ev,i}^{dis,req}=[SOC_{ev,i}^{exp}-SOC_{ev,i}(t)+P_{ev,i}^{dis,rt}\Delta T/(\eta_{ev,i}^{dis}E_{ev,i})]\cdot E_{ev,i}/(\eta_{ev,i}^{chg}P_{ev,i}^{chg,rt}) \tag{8}$$

B. V2G Control Strategy for Aggregated EVs

A hierarchical framework for coordinated charging and discharging of EVs depicted in Fig. 1 consists of three levels: dispatching center level, EVA level, and EV level. As an intermediary between the dispatching center and EV users, the EVA exchanges information with the dispatching center and realizes orderly charging and discharging management of all EVs in its serving zone.

The specific process of V2G control strategy for aggregated EVs to participate in the flexibility improvement of AC-MTDC distribution systems is presented as follows.

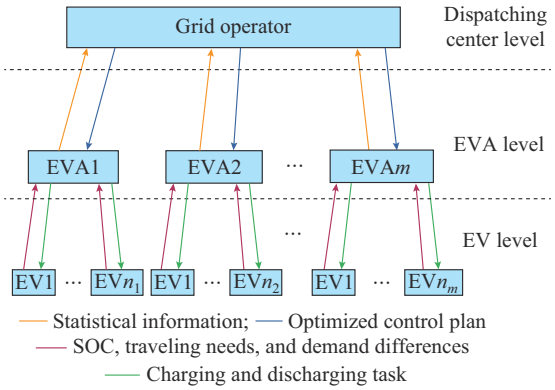

Fig. 1. Hierarchical framework for coordinated charging and discharging of EVs.

1) Data collection. EVs are connected to the power grid through smart charging stations. Once an EV arrives at the smart charging port, its battery capacity and initial SOC can be obtained from the battery management system (BMS) on board. In addition, EV user is required to indicate his/her expected SOC, expected departure time, participation willingness, and so on.

2) Data processing and uploading. According to current status of SOC, traveling needs, and demand differences of EV users, the EVA models the charging and discharging process of each EV and divides all EVs into three groups: charging group, shiftable charging group, and discharging group. The charging group includes all rigid EVs, shiftable EVs, and schedulable EVs that must be charged at time t. The shiftable charging group incorporates shiftable and schedulable EVs whose charging demands can be shifted at time t. Besides, the discharging group contains schedulable EVs that can inject power into the grid at time t.

Then, the EVA sums up charging power of all EVs in charging group and gets the basic charging demand $P_C(t)$ at time t:

$$P_C(t)=\sum_{i\in\Omega_{chg}}P_{ev,i}^{chg}(t) \tag{9}$$

For shiftable charging group, EVA calculates the number of EVs that can be shifted with constant power at time t. As for EVs that cannot be shifted with constant power, the EVA divides them into several groups and counts the total shiftable power of each group. Besides, for discharging group, the EVA counts the total number of EVs at time t. After that, the EVA reports statistical information to the dispatching center via bi-directional communication lines.

3) System optimization. The dispatching center integrates all the information to evaluate and predict the state of power grid. It then optimizes the power flow by coordinating all flexible resources. After that, the dispatching center sends the optimized control plan back to EVA.

4) Charging and discharging management. EVA formulates the charging and discharging plan and issues the charging and discharging task to each EV smart charging port based on the latest control plan. Then, each EV smart charging port charges and discharges EVs automatically.

III. Optimal Flexible Dispatching of AC-MTDC Distribution Systems

A. Flexibility Evaluation Indexes

System flexibility is affected by both flexibility supply and network transfer congestions, and thus FSA and NTM indexes defined in [14] are adopted here to evaluate the system flexibility.

The FSA index can be used to assess if power system has adequate flexibility supply. It can be determined by [14]:

$$FSA(t)=\left(\frac{S_{SA}^{up}(t)F_{SA}^{up}(t)}{P_{NL}(t+\Delta T)}+\frac{S_{SA}^{dn}(t)F_{SA}^{dn}(t)}{P_{NL}(t+\Delta T)}\right)\times 100\% \tag{10}$$

$$\begin{cases} S_{SA}^{up}(t)=1, S_{SA}^{dn}(t)=0 & P_{NL}(t+\Delta T)-P_{NL}(t)>0 \\ S_{SA}^{up}(t)=0, S_{SA}^{dn}(t)=1 & P_{NL}(t)-P_{NL}(t+\Delta T)>0 \end{cases} \tag{11}$$

$$\begin{cases} F_{SA}^{up}(t)=F_{sup}^{up}(t,\Delta T)-F_{de}^{up}(t)-F_{sup,rev}^{up}(t,\Delta T) \\ F_{SA}^{dn}(t)=F_{sup}^{dn}(t,\Delta T)-F_{de}^{dn}(t)-F_{sup,rev}^{dn}(t,\Delta T) \end{cases} \tag{12}$$

$F_{sup}^{up}(t,\Delta T)$ and $F_{sup}^{dn}(t,\Delta T)$ can be calculated as:

$$\begin{cases} F_{sup}^{up}(t,\Delta T)=\sum\limits_{i\in\Omega_{CDG}}F_{CDG,i}^{up}(t,\Delta T)+\sum\limits_{i\in\Omega_{ESS}}F_{ESS,i}^{up}(t,\Delta T)+ \\ \qquad\sum\limits_{i\in\Omega_{SYS}}F_{Grid,i}^{up}(t,\Delta T)+\sum\limits_{i\in\Omega_{EVA}}F_{EVA,i}^{up}(t,\Delta T) \\ F_{sup}^{dn}(t,\Delta T)=\sum\limits_{i\in\Omega_{CDG}}F_{CDG,i}^{dn}(t,\Delta T)+\sum\limits_{i\in\Omega_{ESS}}F_{ESS,i}^{dn}(t,\Delta T)+ \\ \qquad\sum\limits_{i\in\Omega_{SYS}}F_{Grid,i}^{dn}(t,\Delta T)+\sum\limits_{i\in\Omega_{EVA}}F_{EVA,i}^{dn}(t,\Delta T) \end{cases} \tag{13}$$

$$\begin{cases} F_{EVA,i}^{up}(t,\Delta T)=\min\left(0,\sum\limits_{i\in\Omega_{sft}}P_{ev,i}^{chg}(t)+\sum\limits_{i\in\Omega_{dis}}P_{ev,i}^{dis}(t)\right) \\ F_{EVA,i}^{dn}(t,\Delta T)=\min\left(0,\sum\limits_{i\in\Omega_{sft}}P_{ev,i}^{chg}(t)\right) \end{cases} \tag{14}$$

The definition and calculation of $F_{CDG,i}^{up}(t,\Delta T)$, $F_{ESS,i}^{up}(t,\Delta T)$, $F_{Grid,i}^{up}(t,\Delta T)$, $F_{CDG,i}^{dn}(t,\Delta T)$, $F_{ESS,i}^{dn}(t,\Delta T)$, and $F_{Grid,i}^{dn}(t,\Delta T)$ can be referred to [14].

The NTM index is adopted to reveal the network transfer capacity of AC-MTDC distribution systems and is defined as [14]:

$$NTM(t)=\min\left(\frac{S_{line,i}^{\max}-S_{line,i}(t)}{S_{line,i}^{\max}},\frac{S_{trsf,i}^{\max}-S_{trsf,i}(t)}{S_{trsf,i}^{\max}},\frac{S_{VSC,i}^{\max}-S_{VSC,i}(t)}{S_{VSC,i}^{\max}}\right)\times 100\% \tag{15}$$

B. Objective Functions

The objective of the proposed dispatching model is to minimize the total operation cost over the dispatching periods. The total operation cost consists of power purchase cost C_{purch}, network loss cost C_{loss}, operation cost C_{opr}, and penalty cost C_{psh}.

$$\min C_{total}=C_{purch}+C_{loss}+C_{opr}+C_{psh} \tag{16}$$

$$C_{purch}=\sum_{t\in T}\sum_{i\in\Omega_{sys}}c_{Grid,i}(t)P_{Grid,i}(t)\Delta T \tag{17}$$

$$C_{loss}=\sum_{t=1}^{T}c_{Grid,i}(t)\left(\sum_{ij\in\Omega_{AC}}r_{ij}I_{ij}^{2}(t)+\sum_{j\in\Omega_{DC}}r_{ij}^{d}(I_{ij}^{d}(t))^{2}\right)\Delta T \tag{18}$$

$$\begin{aligned} C_{opr}=&C_{WT,opr}+C_{PV,opr}+C_{CDG,opr}+C_{ESS,opr}+C_{EVA,comp}= \\ &\sum_{t\in T}\sum_{i\in\Omega_{WT}}c_{WT}P_{WT,i}(t)\Delta T+\sum_{t\in T}\sum_{i\in\Omega_{PV}}c_{PV}P_{PV,i}(t)\Delta T+ \\ &\sum_{t\in T}\sum_{i\in\Omega_{CDG}}(c_{CDG,i}P_{CDG,i}(t)\Delta T+c_{CDG,i}^{up}\alpha_{CDG,i}^{up}(t)+c_{CDG,i}^{dn}\alpha_{CDG,i}^{dn}(t))+ \\ &\sum_{t\in T}\sum_{i\in\Omega_{ESS}}c_{ESS}(\alpha_{ESS,i}^{chg}(t)P_{ESS,i}^{chg}(t)+\alpha_{ESS,i}^{dis}(t)P_{ESS,i}^{dis}(t))\Delta T+ \\ &\sum_{t\in T}\sum_{i\in\Omega_{sft}}c_{EV,sft}P_{ev,i}^{chg}(t)\Delta T+\sum_{t\in T}\sum_{i\in\Omega_{dis}}c_{EV,dis}P_{ev,i}^{dis}(t)\Delta T \end{aligned} \tag{19}$$

$$\begin{aligned} C_{psh}=&C_{WT,psh}+C_{PV,psh}+C_{LD,psh}=\sum_{t\in T}\sum_{i\in\Omega_{WT}}c_{WT,psh}\Delta P_{WT,i}(t)\Delta T+ \\ &\sum_{t\in T}\sum_{i\in\Omega_{PV}}c_{PV,psh}\Delta P_{PV,i}(t)\Delta T+\sum_{t\in T}\sum_{i\in\Omega_{LD}}c_{LD,psh}\Delta P_{LD,i}(t)\Delta T \end{aligned} \tag{20}$$

Equation (17) is the cost of the electricity purchased from the superior grid. The network loss cost is determined by (18). The operation cost is given by the sum of the cost of power produced by wind turbines (WTs), photovoltaic (PV) units, CDGs, ESSs, and aggregated EVs as in (19) [38]. Besides, penalty fees for power curtailment of WT, PV unit, and load are calculated in (20) [39]. Moreover, it should be noted that (17) can be adapted to any pricing scheme, such as flat rate pricing scheme, time-of-use (TOU) pricing scheme, and prediction-of-use (POU) pricing scheme.

C. Constraints

To ensure a safe and stable operation of AC-MTDC distribution systems, the flexibility improvement dispatching should be solved under several constraints, including AC/DC load flow constraints, flexible resources constraints, flexibility constraints, and system operation constraints. The AC/DC load flow constraints, EV and VSC operation constraints, and flexibility constraints are defined as:

$$\begin{cases} P_{j}^{inj}(t)=V_{i}(t)\sum\limits_{j\in i}V_{j}(t)(G_{ij}\cos\theta_{ij}(t)+B_{ij}\sin\theta_{ij}(t)) \\ Q_{j}^{inj}(t)=V_{i}(t)\sum\limits_{j\in i}V_{j}(t)(G_{ij}\sin\theta_{ij}(t)-B_{ij}\cos\theta_{ij}(t)) \end{cases} \tag{21}$$

$$P_{j}^{d,inj}(t)=V_{i}^{d}(t)\sum_{j\in i}V_{j}^{d}(t)G_{ij}^{d} \tag{22}$$

$$\begin{cases} P_{j}^{inj}(t)=\sum\limits_{i\in\psi_S(j)}P_{Grid,i}(t)+\sum\limits_{i\in\psi_G(j)}P_{CDG,i}(t)+\sum\limits_{i\in\psi_W(j)}P_{WT,i}(t)+ \\ \qquad\sum\limits_{i\in\psi_P(j)}P_{PV,i}(t)+\sum\limits_{i\in\psi_E(j)}(P_{ESS,i}^{dis}(t)-P_{ESS,i}^{chg}(t))+ \\ \qquad\sum\limits_{i\in\psi_A(j)}(P_{EVA,i}^{dis}(t)-P_{EVA,i}^{chg}(t))-\sum\limits_{i\in\psi_L(j)}P_{LD,i}(t)-\sum\limits_{i\in\psi_V(j)}P_{VSC,i}(t) \\ Q_{j}^{inj}(t)=\sum\limits_{i\in\psi_S(j)}Q_{Grid,i}(t)+\sum\limits_{i\in\psi_G(j)}Q_{CDG,i}(t)-\sum\limits_{i\in\psi_L(j)}Q_{LD,i}(t)- \\ \qquad\sum\limits_{i\in\psi_V(j)}Q_{VSC,i}(t) \end{cases} \tag{23}$$

$$P_j^{d,inj}(t)=\sum_{i\in\psi_G^d(j)}P_{CDG,i}(t)+\sum_{i\in\psi_W^d(j)}P_{WT,i}(t)+\sum_{i\in\psi_P^d(j)}P_{PV,i}(t)+\sum_{i\in\psi_E^d(j)}(P_{ESS,i}^{dis}(t)-P_{ESS,i}^{chg}(t))+\sum_{i\in\psi_A^d(j)}(P_{EVA,i}^{dis}(t)-P_{EVA,i}^{chg}(t))-\sum_{i\in\psi_L^d(j)}P_{LD,i}(t)+\sum_{i\in\psi_V^d(j)}P_{VSC,i}(t) \quad (24)$$

$$V_{VSC,i}(t)=\frac{\mu}{\sqrt{2}}M_{VSC,i}V_{VSC,i}^d(t) \quad (25)$$

$$\begin{cases}V_{VSC,i}^d(t)=V_{VSC,i}^{d,ref} & \text{for slack bus}\\ P_{VSC,i}(t)=P_{VSC,i}^{ref} & \text{for slave bus}\end{cases} \quad (26)$$

$$\begin{cases}Q_{VSC,i}(t)=Q_{VSC,i}^{ref} & \text{for constant } Q \text{ control}\\ V_{VSC,i}(t)=V_{VSC,i}^{ref} & \text{for constant } V \text{ control}\end{cases} \quad (27)$$

$$0\le P_{ev,i}^{chg}(t)\le P_{ev,i}^{chg,rt} \quad (28)$$

$$0\le P_{ev,i}^{dis}(t)\le P_{ev,i}^{dis,rt} \quad (29)$$

$$SOC_{ev,i}^{exp}\le SOC_{ev,i}(T_{ev,i}^{leav})\le SOC_{ev,i}^{\max} \quad (30)$$

$$0\le\alpha_{ev,i}^{chg}(t)+\alpha_{ev,i}^{dis}(t)\le 1 \quad (31)$$

$$\sum_{t=1}^{T}(\alpha_{ev,i}^{chg}(t)+\alpha_{ev,i}^{dis}(t))\le C_{ev,i}^{cnv,\max} \quad (32)$$

$$\sqrt{P_{VSC,i}^2(t)+Q_{VSC,i}^2(t)}\le S_{VSC,i}^{\max} \quad (33)$$

$$Q_{VSC,i}^{\min}\le Q_{VSC,i}(t)\le Q_{VSC,i}^{\max} \quad (34)$$

$$FSA(t)>0 \quad (35)$$

$$NTM(t)>0 \quad (36)$$

The power flow constraints and VSC models for AC-MTDC distribution system are described by (21)-(27) [40]. The operational constraints for EV battery are given by (28)-(32). The transfer capacity constraint and reactive power constraint of VSC are determined in (33) and (34), respectively. Besides, flexibility supply constraint and network transfer capacity constraint are given by (35) and (36), respectively. Moreover, system operation constraints, CDG operation constraints, substation operation constraints, and ESS operation constraints can be referred to [14].

D. Solved Algorithm

The flexibility of AC-MTDC distribution system can be promoted by collaboration of VSCs, aggregated EVs, ESSs, and CDGs. In this proposed dispatching method, control variables consist of active power (or DC voltage) and reactive power (or AC voltage) of each VSC, numbers of shiftable charging and discharging EVs, charging and discharging power of each ESS, as well as state variable and active/reactive power of each CDG. Thus, the optimal flexible dispatching model is a large-scale mixed-integer optimization problem in the mathematical form, which can be settled by an improved genetic algorithm [41], [42]. The C++ code of the proposed dispatching method is compiled in Microsoft Visual Studio 2015.

IV. Case Study

A. Basic Data

An AC-MTDC distribution system in [14] is adopted here to demonstrate the effectiveness of this optimal dispatching method. The topology of this AC-MTDC distribution system is given in Fig. 2. Parameters of the system in detail can be referred to [14]. There are seven PVs, seven ESSs, eight WTs, four CDGs, and five EV parking lots in this system. The five EV parking lots are located at buses 5, 12, 20, 30, and 41, respectively.

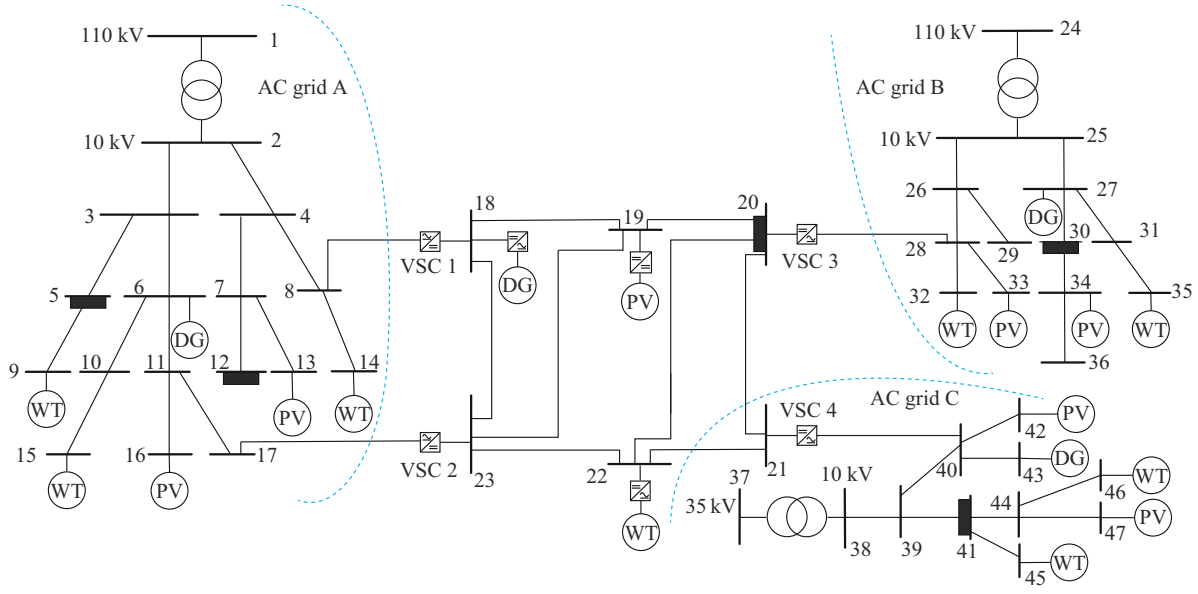

Fig. 2. Topology of an AC-MTDC distribution system.

The simulation interval is set to be 1 hour, and the dispatching period is from 06:00 a.m. to 06:00 a.m. the next morning. The daily load demand curves, power outputs of WTs and PVs in each sub-grid, technical parameters of each substation, CDG, and ESS, as well as the TOU price can be seen in [14]. Suppose that the system has 1000 EVs. Techni-

cal parameters of EV battery are listed in Appendix A Table AI. The arrival time and expected departure time of EVs obey the probability distributions depicted in Appendix A Fig. A1. Moreover, the arrival SOC and expected SOC of EVs follow the probability distributions given in Appendix A Fig. A2.

The maintenance costs of WT and PV are set to be 0.055 ¥/kWh and 0.035 ¥/kWh, respectively. The penalty costs for power curtailment and load shedding are considered to be 1.58 ¥/kWh and 1.98 ¥/kWh, respectively. In addition, the compensation costs of all EVs for providing load shifting and discharging services are considered to be 0.6 and 1.2 times of TOU electricity price, respectively.

B. Optimal Dispatching Results

To illustrate the feasibility and rationality of this optimal dispatching method, and to study the impact of CDG, ESS, aggregated EVs, and VSC on system flexibility, the following five cases are set up.

1) Case A1: the system does not incorporate EVs and only the optimal control of VSC is considered.

2) Case A2: all EVs are rigid EVs and only the optimal control of VSC is considered.

3) Case A3: aggregated EVs and the optimal control of VSC are considered. The ratio among rigid EVs, shiftable EVs, and schedulable EVs is set to be 5:2:3.

4) Case A4: the effect of aggregated EVs and ESS on case A3 is investigated.

5) Case A5: the cooperation effect of all flexible resources on case A3 is investigated.

The optimal dispatching results of these five cases are summarized in Table I.

TABLE I
OPTIMAL DISPATCHING RESULTS OF CASES A1-A5

Case	Total operation cost (¥)	Curtailment (MW)	Load shedding (MW)	Average FSA (%)	Average NTM (%)
A1	129403.5	2.234	2.012	7.281	34.35
A2	145159.6	3.065	3.953	4.885	28.52
A3	141270.3	1.474	2.176	8.423	28.86
A4	139229.2	1.238	1.397	9.560	31.21
A5	135563.0	0	0	23.440	34.52

From Table I, we can see that in case A1, system load demand is the lowest since EV loads are not considered, thus the system has the lowest operation cost. However, system flexibility in case A1 is insufficient, leading to renewable power curtailment and load shedding. Besides, since the system load and power flow are not heavy after optimization, the value of average NTM in case A1 is high, but the value of average FSA is low. In case A2, rigid EVs are taken into consideration. The disordered charging of rigid EVs will deteriorate the operating condition of power grid and call for more flexibility. Compared with the other four cases, case A2 has the highest system cost and power abandonment of PV, WT, and load, whereas it has the lowest average FSA and NTM.

Aggregated EVs are taken part in demand responses in case A3. By orderly charging and discharging of EVs, system flexibility has been improved. The average FSA is increased and renewable power curtailment is reduced as compared to case A1. Compared with case A2, system cost and power abandonment of PV, WT, and load are reduced, whereas values of average FSA and NTM are promoted. With the cooperation of EVs and ESSs, system flexibility in case A4 is improved in comparison with cases A1-A3.

In case A5, system flexibility is further promoted. During the whole dispatching period, no power abandonment of PV, WT, and load occurs. Compared with the other four cases, its average FSA and NTM have been improved. Moreover, system operation cost is reduced too. In comparison with cases A2-A4, the operation cost of case A5 is reduced by 6.61%, 4.04%, and 2.63%, respectively. These results demonstrate that comprehensive optimization of multiple flexibility resources is capable of promoting system flexibility, increasing utilization rate of PV and WT power, reducing load abandonment, and cutting down operation cost.

Figure 3 illustrates the optimal dispatching results of case A5. The system is capable of making full use of electricity from WTs and PVs. Besides, CDGs turn on to work during peak demand periods (09:00-12:00 and 18:00-21:00). They decrease power output during low demand periods (13:00 and 22:00-23:00), and shut down during other periods. In addition, ESSs are discharged in periods 09:00-10:00 and 18:00-19:00 when net load rises severely. They are charged during low pricing periods 02:00-04:00, 13:00-15:00, and 21:00-24:00 when net load declines sharply.

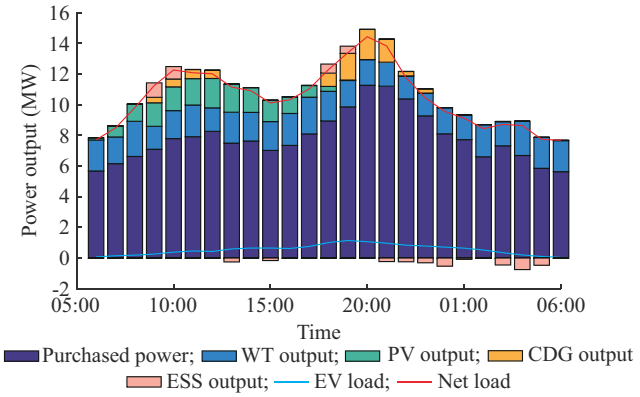

Fig. 3. Optimal dispatching results of case A5.

C. Effective of Proposed Dispatching Method

To demonstrate the validity of the proposed dispatching method (P0), two reference methods are adopted for comparison. The reference method one (R1) in [34] optimizes the operation cost but does not consider flexibility, whereas the reference method two (R2) in [31] optimizes the charging cost and grid losses to get benefit for customers and aggregators. Calculation results of these three methods are listed in Table II.

The results in Table II show that R1 only optimizes the system operation cost, leading to load shedding during peak periods. In addition, R2 optimizes the EV user cost and has the lowest EV user cost. However, the dispatching optimization of R2 is based on the perspective of EV users rather than distribution system, resulting in a large power abandon-

ment of WT, PV, and load. The operation cost, system total cost, power curtailment of WT, PV, and load with R2 are the highest. P0 incorporates flexibility constraints in its model. During each dispatching period, P0 takes flexibility requirements of next dispatching period into account and reserves flexibility supply for the next dispatching period previously. In this way, P0 can better deal with fluctuations and reduce curtailment. Compared with R1 and R2, P0 has the lowest system operation cost and total cost. Besides, there is no power curtailment and load shedding. These results demonstrate that P0 is better than R1 and R2.

TABLE II
CALCULATION RESULTS OF DIFFERENT METHODS

Method	System operation cost (¥)	EV user cost (¥)	Total cost (¥)	Curtailment (MW)	Load shedding (MW)
P0	135940.7	4507.9	140448.5	0	0
R1	137829.9	4517.3	142347.2	0	0.90923
R2	147169.2	4226.6	151395.8	1.35579	1.55768

D. Effect of EV Users' Willingness on Dispatching Results

To study the role of EV users' demand differences in promoting system flexibility, five cases are set up as follows.

1) Case B1: all EVs are rigid types.

2) Case B2: the ratio among rigid EVs, shiftable EVs, and schedulable EVs is 7:1:2.

3) Case B3: the ratio among rigid EVs, shiftable EVs, and schedulable EVs is 5:2:3.

4) Case B4: the ratio among rigid EVs, shiftable EVs, and schedulable EVs is 3:3:4.

5) Case B5: all EVs are schedulable types.

After optimization, optimal dispatching results of cases B1-B5 are obtained and compared in Table III. From Table III, we can observe that in case B1, all EVs are rigid loads and immediately charged as soon as they are plugged in, resulting in load shedding during peak period 20: 00. Compared with cases B2-B5, case B1 has the highest operation cost and the lowest values of average FSA and NTM. Besides, system flexibility is sufficient in cases B2-B5. Meanwhile, as the dispatchable rate of EVs increases, the values of average FSA and NTM increase, indicating that the system flexibility is enhanced. Moreover, the operation costs in cases B2-B5 have been gradually reduced as well. Considering that not all EV users will participate in demand response in the real world, the results of cases B2-B5 demonstrate that better dispatching results can be obtained when the dispatchable rate of EVs reaches 50%.

TABLE III
OPTIMAL DISPATCHING RESULTS OF CASES B1-B5

Case	Total operation cost (¥)	Curtailment (MW)	Load shedding (MW)	Average FSA (%)	Average NTM (%)
B1	137451.9	0	0.88205	20.41	24.39
B2	136312.8	0	0	22.75	24.85
B3	135563.0	0	0	23.44	34.52
B4	135476.8	0	0	24.90	35.35
B5	135416.7	0	0	25.67	36.30

The total EV load curves and total system net load curves of cases B1-B5 are demonstrated in Fig. 4(a) and (b), respectively. Note that the total EV load curves and total system net load curves of case B1 reach the maximum values during peak period 20: 00 and then drop sharply. This reveals that rigid EVs in case B1 deteriorate the total system net load curve, leading to a higher requirement for flexibility during peak periods. Compared with case B1, case B2 reduces the total system net load during peak period 20: 00 by shifting parts of EV loads to off-peak periods. Moreover, as the dispatchable rate of EV increases, more EVs can be shifted to off-peak periods in cases B3-B5. In this way, the total EV load curves and total system net load curves can be smoothed and the requirement for flexibility during peak periods can be reduced as well.

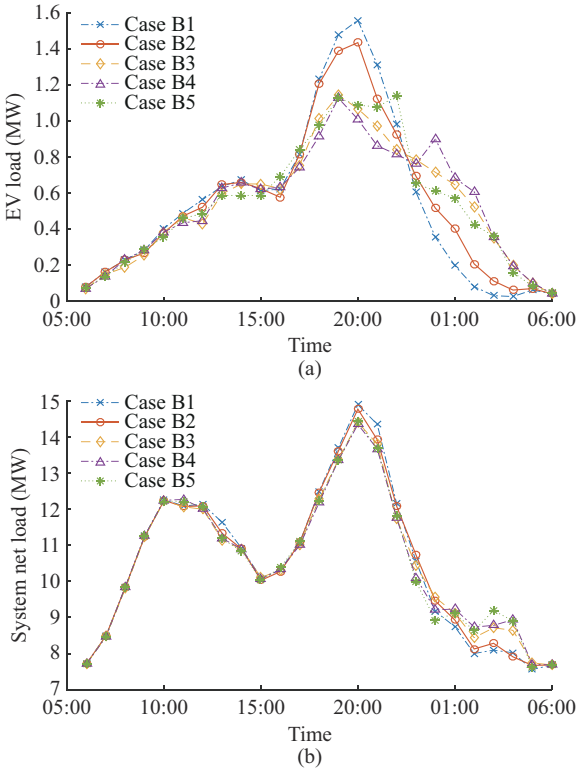

Fig. 4. Total EV load curves and total system net load curves of cases B1-B5. (a) Total EV load curves. (b) Total system net load curves.

E. Impact of EV Penetration on Dispatching Results

In order to analyze the impact of EV penetration on system flexibility, four cases are adopted considering different numbers of EVs with a ratio of 5:2:3 for rigid EVs, shiftable EVs, and schedulable EVs.

1) Case C1: total number of EVs connected to the grid is 1000.

2) Case C2: total number of EVs connected to the grid is 1500.

3) Case C3: total number of EVs connected to the grid is 2000.

4) Case C4: total number of EVs connected to the grid is 2500.

The optimal dispatching results of cases C1-C4 are illustrated in Table IV.

TABLE IV
OPTIMAL DISPATCHING RESULTS OF CASES C1-C4

Case	Total operation cost (¥)	Curtailment (MW)	Load shedding (MW)	Average FSA (%)	Average NTM (%)
C1	135563.0	0	0	23.44	34.50
C2	142176.8	0	0	23.96	32.30
C3	148378.5	0	0	23.82	31.11
C4	157139.7	0	0.87161	22.52	26.40

The results in Table IV indicate that the total operation cost increases accordingly with the increase in EV penetration. Besides, the value of average NTM decreases with the increase of EV penetration. However, the values of average FSA in cases C1-C3 are close to each other and larger than those in case C4. Moreover, load shedding happens in case C4 because of upward flexibility supply insufficiency during peak periods. These results imply that the increase in EV penetration can provide sufficient flexibility to the grid, but too many EVs connected to the grid will increase total load demand, which may lead to load shedding during peak periods. Gradually increasing the number of plug-in EVs, the maximum number of EVs that the test system can accommodate is 2065.

In addition, the total EV load curves and total system net load curves of cases C1-C4 are illustrated in Fig. 5(a) and (b), respectively. The results demonstrate that as the EV penetration increases, the total EV load increases. Meanwhile, the total system net load increases accordingly with the growing EV load as well.

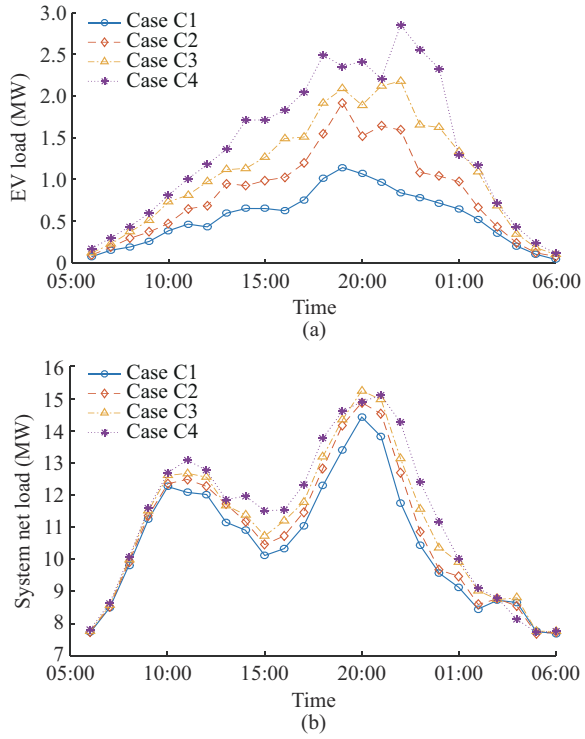

Fig. 5. Total EV load curves and total system net load curves of cases C1-C4. (a) Total EV load curves. (b) Total system net load curves.

V. CONCLUSION

An optimal flexible dispatching method is put forward to promote the flexibility of AC-MTDC distribution systems. The proposed method includes a charging and discharging model of one EV considering users' demand differences and a V2G control strategy for aggregated EVs to take part in the flexibility promotion of distribution systems. Case study demonstrates the merits and effectiveness of the optimal dispatching method. Results indicate that the proposed optimal dispatching method is able to enhance the flexibility of AC-MTDC distribution systems by comprehensively scheduling CDGs, ESSs, aggregated EVs, and VSCs. Some important conclusions have been drawn, as summarized below.

1) EV charging and discharging model proposed in this paper is more realistic because it comprehensively considers the demand differences and traveling needs of EV users. Besides, with the V2G control strategy provided in this paper, aggregated EVs can effectively provide flexibility supply to distribution system.

2) The proposed optimal dispatching method is capable of effectively improving system flexibility, reducing curtailment of WT and PV power, reducing load abandonment, and cutting down system cost.

3) System flexibility can be improved as the dispatchable ratio of EV increases. Moreover, an increase in EV penetration can provide sufficient flexibility to the grid, but too many EVs connected to the grid will increase the total load demand, which may lead to load shedding during peak periods.

APPENDIX A

TABLE AI
OPERATION PARAMETERS OF EV BATTERY

E_{ev} (kWh)	$P_{ev}^{chg,rt}$ (kW)	$P_{ev}^{dischg,rt}$ (kW)	η_{ev}^{chg}	η_{ev}^{dischg}	$SOC_{ev,i}^{\max}$	$SOC_{ev,i}^{\min}$	$SOC_{ev,i}^{thd}$
25	5	5	0.9	0.9	0.1	0.9	0.4

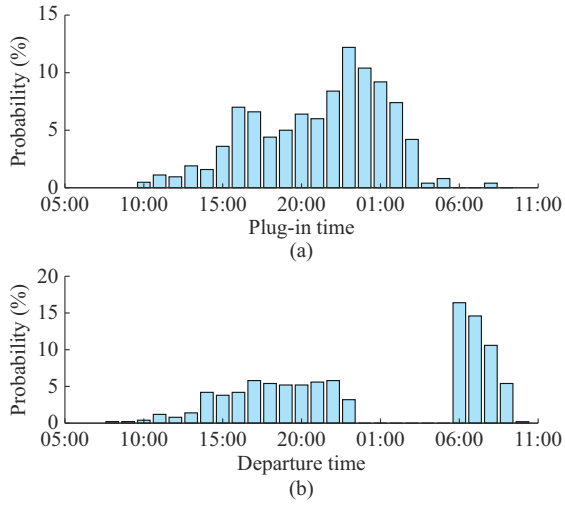

Fig. A1. Probability distribution of plug-in time and departure time of EVs. (a) Plug-in time. (b) Departure time.

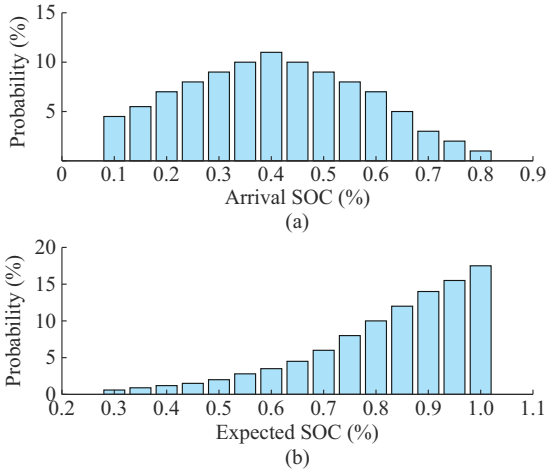

Fig. A2. Probability distribution of arrival SOC and expected SOC of EVs. (a) Arrival SOC. (b) Expected SOC.

REFERENCES

[1] R. You and X. Lu, "Voltage unbalance compensation in distribution feeders using soft open points," *Journal of Modern Power Systems and Clean Energy*, vol. 10, no. 4, pp. 1000-1008, Jul. 2022.

[2] S. Naghdalian, T. Amraee, S. Kamali *et al*., "Stochastic network-constrained unit commitment to determine flexible ramp reserve for handling wind power and demand uncertainties," *IEEE Transactions on Industrial Informatics*, vol. 16, no. 7, pp. 4580-4591, Jul. 2020.

[3] P. Chen, W. Zhao, X. Chen *et al*., "An impedance-based parameter design method for active damping of load converter station in MTDC distribution system," *Journal of Modern Power Systems and Clean Energy*, vol. 10, no. 5, pp. 1423-1436, Sept. 2022.

[4] B. Mohandes, M. S. E. Moursi, N. Hatziargyriou *et al.*, "A review of power system flexibility with high penetration of renewables," *IEEE Transactions on Power Systems*, vol. 34, no. 4, pp. 3140-3155, Jul. 2019.

[5] E. Heydarian-Forushani, M. E. H. Golshan, and P. Siano, "Evaluating the operational flexibility of generation mixture with an innovative techno-economic measure," *IEEE Transactions on Power Systems*, vol. 33, no. 2, pp. 2205-2218, Mar. 2018.

[6] K. Wang, R. Yin, and L. Yao, "A two-layer framework for quantifying demand response flexibility at bulk supply points," *IEEE Transactions on Smart Grid*, vol. 9, no. 4, pp. 3616-3627, Jul. 2018.

[7] Y. Shi, S. Dong, C. Guo *et al*., "Enhancing the flexibility of storage integrated power system by multi-stage robust dispatch," *IEEE Transactions on Power Systems*, vol. 36, no. 3, pp. 2314-2322, May 2021.

[8] A. Majzoobi and A. Khodaei, "Application of microgrids in supporting distribution grid flexibility," *IEEE Transactions on Power Systems*, vol. 32, no. 5, pp. 3660-3669, Sept. 2017.

[9] A. Nikoobakht, M. Mardaneh, J. Aghaei *et al*., "Flexible power system operation accommodating uncertain wind power generation using transmission topology control: an improved linearised AC SCUC model," *IET Generation, Transmission & Distribution*, vol. 11, pp. 142-153, Jan. 2017.

[10] S. Dalhues, Y. Zhou, O. Pohl *et al*., "Research and practice of flexibility in distribution systems: a review," *CSEE Journal of Power and Energy Systems*, vol. 5, no. 3, pp. 285-294, Sept. 2019.

[11] H. Nosair and F. Bouffard, "Flexibility envelopes for power system operational planning," *IEEE Transactions on Sustainable Energy*, vol. 6, no. 3, pp. 800-809, Jul. 2015.

[12] E. Lannoye, D. Flynn, and M. O'Malley, "Transmission, variable generation, and power system flexibility," *IEEE Transactions on Power Systems*, vol. 30, no. 1, pp. 57-66, Jan. 2015.

[13] A. A. Thatte and L. Xie, "A metric and market construct of inter-temporal flexibility in time-coupled economic dispatch," *IEEE Transactions on Power Systems*, vol. 31, no. 5, pp. 3437-3446, Sept. 2016.

[14] X. Jiang, S. Wang, Q. Zhao *et al*., "Exploiting the operational flexibility of AC-MTDC distribution system considering various flexible resources," *International Journal of Electrical Power & Energy Systems*, vol. 148, p. 108842, Jan. 2023.

[15] L. Nan, C. Uckun, E. Constantinescu *et al*., "Flexible operation of batteries in power system scheduling with renewable energy," *IEEE Transactions on Sustainable Energy*, vol. 7, no. 2, pp. 685-696, Apr. 2016.

[16] S. Gottwalt, J. Garttner, H. Schmeck *et al*., "Modeling and valuation of residential demand flexibility for renewable energy integration," *IEEE Transactions on Smart Grid*, vol. 8, no. 6, pp. 2565-2574, Nov. 2017.

[17] Y. Shi, S. Dong, C. Guo *et al*., "Enhancing the flexibility of storage integrated power system by multi-stage robust dispatch," *IEEE Transactions on Power Systems*, vol. 36, no. 3, pp. 2314-2322, May 2021.

[18] H. Wu, M. Shahidehpour, A. Alabdulwahab *et al*., "Thermal generation flexibility with ramping cost and hourly demand response in stochastic security-constrained scheduling of variable energy sources," *IEEE Transactions on Power Systems*, vol. 30, no. 6, pp. 2955-2964, Nov. 2015.

[19] A. Nikoobakht, J. Aghaei, M. Shafie-Khah *et al*., "Assessing increased flexibility of energy storage and demand response to accommodate a high penetration of renewable energy sources," *IEEE Transactions on Sustainable Energy*, vol. 10, no. 2, pp. 659-669, Apr. 2019.

[20] S. Gao, S. Liu, Y. Liu *et al*., "Flexible and economic dispatching of AC/DC distribution networks considering uncertainty of wind power," *IEEE Access*, vol. 7, pp. 100051-100065, Aug. 2019.

[21] H. Huang, M. Zhou, S. Zhang *et al*., "Exploiting the operational flexibility of wind integrated hybrid AC/DC power systems," *IEEE Transactions on Power Systems*, vol. 36, no. 1, pp. 818-826, Jan. 2021.

[22] Z. Fotouhi, M. R. Hashemi, H. Narimani *et al*., "A general model for EV drivers' charging behavior," *IEEE Transactions on Vehicular Technology*, vol. 68, no. 8, pp. 7368-7382, Aug. 2019.

[23] C. Wei, J. Xu, S. Liao *et al*., "Aggregation and scheduling models for electric vehicles in distribution networks considering power fluctuations and load rebound," *IEEE Transactions on Sustainable Energy*, vol. 11, no. 4, pp. 2755-2764, Oct. 2020.

[24] H. Liu, J. Qi, J. Wang *et al*., "EV dispatch control for supplementary frequency regulation considering the expectation of EV owners," *IEEE Transactions on Smart Grid*, vol. 9, no. 4, pp. 3763-3772, Jul. 2018.

[25] I. Pavic, T. Capuder, and I. Kuzle, "A comprehensive approach for maximizing flexibility benefits of electric vehicles," *IEEE System Journal*, vol. 12, no. 3, pp. 2882-2893, Sept. 2018.

[26] M. Raoofat, M. Saad, S. Lefebvre *et al*., "Wind power smoothing using demand response of electric vehicles," *International Journal of Electrical Power & Energy Systems*, vol. 99, pp. 164-174, Jul. 2018.

[27] R. Shi, S. Li, P. Zhang *et al*., "Integration of renewable energy sources and electric vehicles in V2G network with adjustable robust optimization," *Renewable Energy*, vol. 153, pp. 1067-1080, Jun. 2020.

[28] Y. Huang, "Day-ahead optimal control of PEV battery storage devices taking into account the voltage regulation of the residential power grid," *IEEE Transactions on Power Systems*, vol. 34, no. 6, pp. 4154-4167, May 2019.

[29] E. Yao, V. W. S. Wong, and R. Schober, "Robust frequency regulation capacity scheduling algorithm for electric vehicles," *IEEE Transactions on Smart Grid*, vol. 8, no. 2, pp. 1-14, Mar. 2016.

[30] I. Pavic, T. Capuder, and I. Kuzle, "Value of flexible electric vehicles in providing spinning reserve services," *Applied Energy*, vol. 157, no. 12, pp. 60-74, Nov. 2015.

[31] S. Sachan and N. Adnan, "Stochastic charging of electric vehicles in smart power distribution grids," *Sustainable Cities and Society*, vol. 40, pp. 91-100, Jul. 2018.

[32] C. Peng, J. Zou, L. Lian *et al*., "An optimal dispatching strategy for V2G aggregator participating in supplementary frequency regulation considering EV driving demand and aggregator's benefits," *Applied Energy*, vol. 190, pp. 591-599, Mar. 2017.

[33] G. Coria, D. Romero-Quete, and A. Romero, "Computational efficient approach to compute a prediction-of-use tariff for coordinating charging of plug-in electric vehicles under uncertainty," *International Journal of Electrical Power and Energy Systems*, vol. 136, pp. 1-12, Mar. 2022.

[34] A. Rabiee, M. Sadeghi, J. Aghaeic *et al*., "Optimal operation of microgrids through simultaneous scheduling of electrical vehicles and responsive loads considering wind and PV units uncertainties," *Renewable and Sustainable Energy Reviews*, vol. 57, pp. 721-739, May 2016.

[35] A. A. Eajal, M. F. Shaaban, K. Ponnambalam *et al*., "Stochastic centralized dispatch scheme for AC/DC hybrid smart distribution systems," *IEEE Transactions on Sustainable Energy*, vol. 7, no. 3, pp. 1046-1059, Jul. 2016.

[36] M. Shafie-Khah, P. Siano, D. Z. Fitiwi *et al*., "An innovative two-level model for electric parking lots in distribution systems with renewable energy," *IEEE Transactions on Smart Grid*, vol. 9, no. 2, pp. 1506-1520, Mar. 2018.

[37] M. Mohiti, H. Monsef, and H. Lesani, "A decentralized robust model for coordinated operation of smart distribution network and electric vehicle aggregators," *Electrical Power and Energy Systems*, vol. 104, pp. 853-867, Jan. 2019.
[38] H. Qiu, W. Gu, X. Xu *et al*., "A historical-correlation-driven robust optimization approach for microgrid dispatch," *IEEE Transactions on Smart Grid*, vol. 12, no. 2, pp. 1135-1148, Mar. 2021.
[39] E. Heydarian-Forushani, M. E. H. Golshan, and P. Siano, "Evaluating the operational flexibility of generation mixture with and innovative techno-economic measure," *IEEE Transactions on Power Systems*, vol. 33, no. 2, pp. 2205-2218, Mar. 2018.
[40] S. Wang, X. Jiang, Q. Zhao *et al*., "Unified load flow calculation for flexible interconnected AC-MTDC distribution system considering control strategy switching with high penetration of DGs," *International Journal of Electrical Power & Energy Systems*, vol. 131, p. 107130, Oct. 2021.
[41] R. Ponciroli, N. E. Stauff, J. Ramsey *et al*., "An improved genetic algorithm approach to the unit commitment/economic dispatch problem," *IEEE Transactions on Power Systems*, vol. 35, no. 5, pp. 4005-4013, Sept. 2020.
[42] M. Yan, H. Hu, Y. Otake *et al*., "Improved adaptive genetic algorithm with sparsity constraint applied to thermal neutron CT reconstruction of two-phase flow," *Measurement Science & Technology*, vol. 29, pp. 1-14, May 2018.

Xingyue Jiang received the B.S. degree in electrical engineering from Tianjin University, Tianjin, China, in 2007, where she is currently pursuing the Ph.D. degree in the School of Electrical and Information Engineering. Her research interests include AC/DC distribution system analysis, grid integration of electric vehicles, and distributed energy resources.

Shouxiang Wang received the B.S. and M.S. degrees in electrical engineering from Shandong University, Jinan, China, in 1995 and 1998, respectively, and the Ph.D. degree in electrical engineering from Tianjin University, Tianjin, China, in 2001. He is currently a Professor at the School of Electrical and Information Engineering, and Deputy Director of the Key Laboratory of Smart Grid of Ministry of Education, Tianjin University. His research interests include distributed generation, microgrid, and smart distribution system.

Qianyu Zhao received the B.S. and M.S. degrees in electrical engineering and control science and engineering from Tiangong University, Tianjin, China, in 2012 and 2015, respectively, and the Ph.D. degree in electrical engineering from Tianjin University, Tianjin, China, in 2020. She is currently an Assistant Professor at the School of Electrical and Information Engineering, Tianjin University. Her research interests include planning, assessment of energy storage and distributed generation, and uncertainty analysis of distribution networks.

Xuan Wang received the B.S. degree in electrical engineering from Shandong University of Technology, Shandong, China, in 2017, and the M.S. degree in electrical engineering from Tianjin University, Tianjin, China, in 2020, where she is currently pursuing the Ph.D. degree in the School of Electrical and Information Engineering. Her research interests include artificial intelligence and integrated energy.